Applications of the Bernoulli wavelet collocation method in the analysis of MHD boundary layer flow of a viscous fluid

S. Kumbinarasaiah[1] · M. P. Preetham[1]

Abstract
This study focuses on the flow of viscous, electrically conducting incompressible fluid over a stretching plate. The Falkner–Skan equation is a nonlinear, third-order boundary value problem. No closed-form solutions are available for this two-point boundary value problem. Here, we developed a new functional matrix of integration using the Bernoulli wavelet and also generated a new technique called Bernoulli wavelet collocation method (BWCM) to solve the nonlinear differential equation that arises in the fluid flow over a stretching plate. The boundary layer model is transformed to a nonlinear ordinary differential equation called the Falkner-Skan type equation using suitable transformation. Using BWCM, we have solved the unbounded governing equations of different types that arise in the MHD boundary-layer flow of a viscous fluid over a stretching plate. Several aspects of this problem are justified using the Haar wavelet and the previously obtained theoretical results. It is observed that the boundary-layer thickness decreases as the pressure gradient and magnetic field parameters increase. The overshoots and undershoots are observed for some particular parameters using BWCM. Furthermore, our research yields dual solutions for some physical parameters, which are investigated for the first time in the literature using the Bernoulli wavelet approach. The nature of the flow problem is discussed through the graphs by varying the physical parameters.

1 Introduction

The boundary layer flow (BLF) of a fluid over a stretching area has many applications in mathematical engineering and other fields, such as condensation of liquid film, aerodynamics, drawing of plastic films, wire drawing, cooling of films or sheets, insulating materials, metallic plates, and conveyor belts, etc., The first work in this field is done by B. C. Sakiadis [1] to examine the BLF on a continuous solid surface. B. K. Datta [2] derived an approximate solution for the Blasius equation using δ-perturbation technique. Abbasbandy [3] used the Adomian decomposition

method (ADM) to solve the Blasius equation. Abbasbandy and T. Hayat [4, 5] gave the solution for MHD Falkner Skan equations by employing the Hankel-Pade and homotopy analysis methods (HAM), respectively. M. Khan et al. [6] proposed a new technique known as the homotopy analysis transform method, a combination of HAM and Laplace decomposition approach, to find an approximate solution for Blasius equations. H. Zeb et al. [7] studied the nature of Non-Newtonian Ferrofluid over a stretching plate using the Runge–Kutta method. T. Anusha et al.[8] provided the exact solution for the MHD of nanofluid over stretching or shrinking plate with mass transpiration and Brinkman

✉ S. Kumbinarasaiah, kumbinarasaiah@gmail.com | [1]Department of Mathematics, Bangalore University, Bengaluru, India.

ratio. S. Liao applied HAM to study incompressible viscous fluid flow over a stretching plate [9, 10] and the MHD flow of non-Newtonian fluid over a stretching sheet[11]. Asaithambi studied the Falkner-Skan problem using the finite difference method [12] and the recursive evaluation of Taylor coefficients [13]. R. B. Kudenatti et al. investigated MHD flow over a stretching plate [14] and with suction and injection [15]. R. B. Kudenatti et al. [16] gave approximate analytical solutions for the equations that arise in the nonlinear stretching surface using the asymptotic function method, method of stretching variables, and Dirichlet series. R. B. Kudenatti [17] proposed the exact solution for BLF over a stretching plate. P. L. Sachdev [18] investigated the Falkner Skan equation by solving exactly. The investigation on heat transfer of incompressible electrically conducting fluid was done by A. Chakrabarti [19] and with a power-law velocity by Chiam [20]. Many researchers have studied MHD stretching sheets in quiescent fluid, micropolar fluids, magneto-convection, nonlinear radiation, and diffusion (M. J. Uddin et al.[21–23]). Some other techniques, such as modified ADM, pade approximation (Hayat et al. [24]), and differential transform method (Rashidi [25]), are employed to study the flow over a stretching sheet.

Here, the boundary layer model is transformed into a nonlinear ordinary differential equation called the Falkner-Skan type equation using suitable transformation. The Falkner–Skan equation, originally derived in 1931 by Falkner and Skan, is of central importance to the fluid mechanics of wall-bounded viscous flows. It is derived from the two-dimensional incompressible Navier–Stokes equations for a one-sided bounded flow using similarity analysis. Its solution describes the form of an external laminar boundary layer in the presence of an adverse or favorable streamwise pressure gradient. Despite the apparent simplicity of the Falkner-Skan equation solving it accurately can be fraught with difficulty; these problems mainly stem from its non-linearity and third-degree order. There are some examples of analytical solutions to the Falkner-Skan equations for special cases, but most studies have focused either on demonstrating a solution's existence and uniqueness or finding a numerical/computational solution for particular boundary-layer conditions.

During the terminating year of the twentieth era, the abundant and philosophical theory of wavelets was created due to the efforts of mathematicians, physicists, and engineers. Wavelet methods have been widely used in image and signal processing, approximation theory, geophysics, and many more. Wavelet-based numerical techniques have become a popular method for solving differential equations. In the latest centuries, much consideration has been dedicated to the newly established approaches for the numerical solution of an equation such approaches include the wavelet methods to solve nonlinear equations arising

in fluid problems [26–38]. Some other techniques, such as Perturbation techniques, are too strongly hooked on "small parameters". Thus, developing some new numerical techniques is advisable, not dependent on small parameters. In this article, we use the Bernoulli wavelet operational method of integration to solve the nonlinear ordinary differential equations. P. Rahimkhani et al. proposed an operational matrix based on Bernoulli wavelets for solving delay differential equations [39] and fractional-order Bernoulli wavelet method to solve pantograph differential equations [40]. Adel and Sabir [41] investigated Lane–Emden pantograph delay differential model using the Bernoulli collocation method. Lal and Kumar [42] numerically investigated Volterra integral equation via the Bernoulli wavelet. A numerical investigation of Volterra Integro-Differential Equations by employing the Bernoulli wavelet method was done by Sahu and Saha Ray [43]. Many researchers have solved nonlinear singular Lane–Emden equations [44], fractional-order differential equations [45], linear and nonlinear problems in the calculus of variations (Hedayati [46]), Fractional Diffusion Wave Equations [47] using the Bernoulli wavelet method. Here, we developed a new operational matrix; using BWCM, we have solved the unbounded governing equations of different types that arise in the MHD BLF of a viscous fluid. Usually, ordinary differential equations (ODEs) describe many physical phenomena in fluid dynamics, mathematical biology, chemical theory, and bio-modeling. Several mathematicians have considered these models in past decades, and many techniques have been developed to describe the above model. But the Falkner Skan type equation is highly nonlinear ODE, so anticipating the exact solution is always impossible. We need to switch to numerical methods to crack such a model. Because of this, we proposed a new novel approach called BWCM to solve the **Falkner–Skan type equation**. The primary purpose of this study is to present and explain a new BWCM for obtaining the numerical solution to nonlinear ODE that cannot be solved exactly. Here, the magnetohydrodynamic BLF of a viscous fluid is considered to analyze the effects of M, β and ϵ of fluid flow. This work aims to solve a nonlinear differential equation governing the magnetohydrodynamic BLF of a viscous fluid using a novel approach called the BWCM. Nonlinear differential equations are solved through this technique and compared with the exact solution and the Haar wavelet solution. Some plots and tables are presented to show the reliability and simplicity of the method. Here, we computed the solution of the Falkner-Skan equation using a wavelet scheme. There are several previously reported many approaches, such as shooting, Taylor series, Runge–Kutta, and other semi-analytic methods. Interestingly, the methods that directly solve the original non-reduced third-order equation are absent from the literature; to our knowledge, this is the first time a continuous wavelet scheme has been presented to find

numerical solutions to the Falkner–Skan equation directly. This approach avoids complicated numerical algorithms and presents valuable information about the numerical behavior of the equation. The accuracy and effectiveness of this approach are established by comparison with published work.

2 Problem formulation

The continuity equation and Navier–Stokes equation for a two-dimensional steady flow of an incompressible viscous fluid in the absence of body force are given by [48]:

$$\nabla \cdot \vec{q} = 0, \tag{1}$$

$$\rho(\vec{q} \cdot \nabla)\vec{q} = -\nabla p + \mu \nabla^2 \vec{q}, \tag{2}$$

where $\vec{q}$ is the velocity, μ is the viscosity, ρ is the density, and p is the pressure.

To find $(\vec{q} \cdot \nabla)\vec{q}, \nabla^2 \vec{q}$:

$$(\vec{q} \cdot \nabla)\vec{q} = \left[(u\,\hat{i} + v\,\hat{j}) \cdot \left(\hat{i}\,\frac{\partial}{\partial x} + \hat{j}\,\frac{\partial}{\partial y}\right)\right](u\,\hat{i} + v\,\hat{j}) = \left(u\,\frac{\partial u}{\partial x} + v\,\frac{\partial u}{\partial y}\right)\hat{i} + \left(u\,\frac{\partial v}{\partial x} + v\,\frac{\partial v}{\partial y}\right)\hat{j}.$$

$$\nabla^2 \vec{q} = \left(\frac{\partial^2}{\partial x^2} + \frac{\partial^2}{\partial y^2}\right)(u\,\hat{i} + v\,\hat{j})$$

$$= \left(\frac{\partial^2 u}{\partial x^2} + \frac{\partial^2 u}{\partial y^2}\right)\hat{i} + \left(\frac{\partial^2 v}{\partial x^2} + \frac{\partial^2 v}{\partial y^2}\right)\hat{j}.$$

With these (1) and (2) becomes,

$$\frac{\partial u}{\partial x} + \frac{\partial v}{\partial y} = 0,$$

$$u\,\frac{\partial u}{\partial x} + v\,\frac{\partial u}{\partial y} = \frac{-1}{\rho}\frac{\partial p}{\partial x} + \frac{\mu}{\rho}\left(\frac{\partial^2 u}{\partial x^2} + \frac{\partial^2 u}{\partial y^2}\right),$$

$$u\,\frac{\partial v}{\partial x} + v\,\frac{\partial v}{\partial y} = \frac{-1}{\rho}\frac{\partial p}{\partial y} + \left(\frac{\partial^2 v}{\partial x^2} + \frac{\partial^2 v}{\partial y^2}\right).$$

$$\Rightarrow \frac{\partial u}{\partial x} + \frac{\partial v}{\partial y} = 0, \tag{3}$$

$$u\,\frac{\partial u}{\partial x} + v\,\frac{\partial u}{\partial y} = \frac{-1}{\rho}\frac{\partial p}{\partial x} + \nu\left(\frac{\partial^2 u}{\partial x^2} + \frac{\partial^2 u}{\partial y^2}\right), \tag{4}$$

$$u\,\frac{\partial v}{\partial x} + v\,\frac{\partial v}{\partial y} = \frac{-1}{\rho}\frac{\partial p}{\partial y} + \nu\left(\frac{\partial^2 v}{\partial x^2} + \frac{\partial^2 v}{\partial y^2}\right), \tag{5}$$

where $\nu = \frac{\mu}{\rho}$ is kinematic viscosity.

To compare the order of magnitude of each term in Eqs. (3),(4),(5), it is more advantageous to put the Eqs. (3),(4),(5) in dimensionless form by letting,

$$x^* = \frac{x}{L}, \; y^* = \frac{y}{\delta}, \; u^* = \frac{u}{U}, \; v^* = \frac{v}{V}, \; t^* = \frac{t}{\frac{L}{U}}, \; p^* = \frac{p}{p_\infty}, \tag{6}$$

where L, δ, U, V, and p_∞ are certain values of the corresponding quantities x, y, u, v, and p. All dimensionless quantities are of order unity.

Using (6) in (3), we get,

$$\frac{U}{L}\frac{\partial u^*}{\partial x^*} + \frac{V}{\delta}\frac{\partial v^*}{\partial y^*} = 0. \tag{7}$$

Integrating Eq. (7), after making use of the condition $(v^*)_{y^*=1} = 1$,

$$\frac{V}{U} = -\frac{\delta}{L}\int_0^1 \frac{\partial u^*}{\partial x^*}\,dy^*. \tag{8}$$

Since the integral in Eq. (8) is of order unity, the order of the velocity ratio $\frac{V}{U}$ is $\frac{\delta}{L}$. Hence $V \ll U$, Using (6) in (4),

$$u^*\frac{\partial u^*}{\partial x^*} + \frac{V}{U}\frac{L}{\delta}\frac{\partial u^*}{\partial y^*} = -\frac{p_\infty}{\rho U^2}\frac{\partial p^*}{\partial x^*} + \frac{1}{Re}\left(\frac{\partial^2 u^*}{\partial x^{*2}} + \frac{L^2}{\delta^2}\frac{\partial^2 u^*}{\partial y^{*2}}\right). \tag{9}$$

Using (6) in (5),

$$\frac{V}{U}u^*\frac{\partial v^*}{\partial x^*} + \frac{V^2}{U^2}\frac{L}{\delta}\frac{\partial v^*}{\partial y^*} = -\frac{L\,p_\infty}{\rho\,\delta\,U^2}\frac{\partial p^*}{\partial x^*} + \frac{1}{Re}\frac{V}{U}\left(\frac{\partial^2 v^*}{\partial x^{*2}} + \frac{L^2}{\delta^2}\frac{\partial^2 v^*}{\partial y^{*2}}\right). \tag{10}$$

where $Re = \frac{UL}{\nu}$ is the Reynolds number $\left(Re \sim \frac{1}{\delta^2}\right)$. Neglecting the terms of order of δ and smaller from Eqs. (9) and (10) and reverting to dimensional variables, we get,

$$u\,\frac{\partial u}{\partial x} + v\,\frac{\partial u}{\partial y} = \frac{-1}{\rho}\frac{\partial p}{\partial x} + \nu\,\frac{\partial^2 u}{\partial y^2}, \tag{11}$$

$$\frac{\partial p}{\partial y} = 0, \tag{12}$$

$$\frac{\partial u}{\partial x} + \frac{\partial v}{\partial y} = 0. \tag{13}$$

Now we will consider a two-dimensional steady and laminar boundary layer flow of an electrically conducting incompressible viscous fluid due to the stretching surface. A magnetic field $B(x)$ is applied to the flow in the direction normal to the stretching surface. The axes x and y are taken along

the boundary-layer flow and to its normal, respectively. Here, the physical properties of the fluid are taken to be constant.

Using the above magnitude analysis along with boundary-layer approximations, we get,

$$\frac{\partial u}{\partial x} + \frac{\partial v}{\partial y} = 0, \tag{14}$$

$$u\frac{\partial u}{\partial x} + v\frac{\partial u}{\partial y} = \frac{-1}{\rho}\frac{dp}{dx} + \nu\frac{\partial^2 u}{\partial y^2} - \frac{\sigma B^2 u}{\rho}. \tag{15}$$

Subjected to the boundary conditions:

$$y = 0: \quad u = U_w(x), \quad v = 0,$$
$$\frac{y}{\delta} \rightarrow \infty: \quad u \rightarrow U_\infty(x). \tag{16}$$

where the velocity components u and v are the streamwise and normal velocity components in directions x and y, respectively, $U_\infty(x)$ is the velocity at the edge of the boundary layer of thickness δ, $U_w(x)$ is the velocity of the bounding surface.

At $y = \delta$, $\frac{\partial u}{\partial y} = 0$, then Eq. (15) reduces to

$$U_\infty\frac{dU_\infty}{dx} + \frac{\sigma B^2 U_\infty}{\rho} = \frac{-1}{\rho}\frac{dp}{dx}. \tag{17}$$

Using (17) in (15),

$$u\frac{\partial u}{\partial x} + v\frac{\partial u}{\partial y} = U_\infty\frac{dU_\infty}{dx} + \nu\frac{\partial^2 u}{\partial y^2} - \frac{\sigma B^2(u - U_\infty)}{\rho}. \tag{18}$$

It is observed that, at the bounding surface, the fluid's velocity will decompose into the mainstream flows either exponentially or algebraically, and that depends on the imposed pressure gradient on the flow. The similarity solutions exist if $U_w(x)$, $U_\infty(x)$, and $B(x)$ obey the following power-law relations

$$U_w(x) = U_{ow}(x)x^n, \quad U_\infty(x) = U_{0\infty}(x)x^n, \quad B(x) = B_0 x^{(n-1)/2}. \tag{19}$$

where U_{ow}, $U_{0\infty}$, B_0 are non-negative constants and n is associated with either non-uniform stretching speed or pressure gradient. The nondimensional coordinate transformation and stream function are introduced [18, 48],

$$\psi = \sqrt{\frac{2\nu x U}{1+n}}f(\eta), \quad \eta = y\sqrt{\frac{(1+n)U}{2\nu x}}. \tag{20}$$

where the stream function $\psi(x, y)$ satisfying the continuity Eq. (14) and is defined as:

$$u = -\frac{\partial\psi}{\partial y}, \quad v = \frac{\partial\psi}{\partial x}. \tag{21}$$

Now, the composite reference velocity U is defined as:

$$U(x) = U_w(x) + U_\infty(x). \tag{22}$$

Using the above transformations, Eqs. (18) and (16) become,

$$f'''(\eta) + f(\eta)f''(\eta) + \beta\left(\in^2 -(f'(\eta))^2\right) + M^2\left(\in -f'(\eta)\right) = 0, \tag{23}$$

$$f(0) = 0, \quad f'(0) = 1 - \in, \quad f'(\infty) = \in. \tag{24}$$

where $\in$ is a composite velocity parameter given by,

$$\in = \frac{U_\infty}{U_w + U_\infty}, \quad U_w + U_\infty \neq 0, \tag{25}$$

$\beta = \frac{2n}{n+1}$ measures the stretch rate of the moving boundary and $M = \sqrt{\frac{2\sigma}{\rho(n+1)U_{0\infty}}}B_0$ is the magnetic parameter (Hartmann number).

3 Preliminaries of Bernoulli wavelet and its properties

The Bernoulli wavelets are defined as [45],

$$\theta_{n,m}(x) = \begin{cases} 2^{\frac{k-1}{2}}\widetilde{b_m}\left(2^{k-1}x - \hat{n}\right), & \frac{-\hat{n}}{2^{k-1}} \leq x < \frac{\hat{n}+1}{2^{k-1}}, \\ 0, Otherwise. \end{cases}$$

with

$$\widetilde{b_m}(x) = \begin{cases} 1, m = 0, \\ \frac{1}{\sqrt{\frac{(-1)^{m-1}(m!)^2}{(2m)!}a_{2m}}}b_m(x), m > 0. \end{cases}$$

where $m = 0, 1, 2, \ldots, M - 1$, $\hat{n} = n - 1$, $n = 1, 2, \ldots, 2^{(k-1)}$.

The coefficient $\frac{1}{\sqrt{\frac{(-1)^{m-1}(m!)^2}{(2m)!}a_{2m}}}$ is for normality, the dilation parameter is $f = 2^{-(k-1)}$ and the translation parameter $g = \hat{n}2^{-(k-1)}$. Here, $b_m(x)$ are the familiar Bernoulli polynomials of order m which can be defined by, $b_m(x) = \sum_{i=0}^{m}\binom{m}{i}a_{m-i}x^i$, where $a_i, i = 0, 1, \ldots, m$ are Bernoulli numbers.

A few Bernoulli numbers are:

$$a0 = 1, a_1 = \frac{-1}{2}, a_2 = \frac{1}{6}, a_4 = \frac{-1}{30},$$
$$a_6 = \frac{1}{42}, a_8 = \frac{-1}{30}, a_{10} = \frac{5}{66}, a_{12} = -\frac{691}{2730},$$
$$a_{14} = \frac{7}{6}, a_{16} = -\frac{3617}{510}, a_{18} = \frac{43867}{798}, \ldots$$

with $a_{2i+1} = 0, i = 1, 2, 3, \ldots$

Few Bernoulli polynomials are given by

$$b_0 = 1, b_1 = -\frac{1}{2} + x, b_2 = \frac{1}{6} - x + x^2, b_3 = \frac{x}{2} - \frac{3x}{2} + x^3,$$

$$b_4 = -\frac{1}{30} + x^2 - 2x^3 + x^4, b_5 = -\frac{x}{6} + \frac{5x^3}{3} - \frac{5x^4}{2} + x^5,$$

$$b_6 = \frac{1}{42} - \frac{x^2}{2} + \frac{5x^4}{2} - 3x^5 + x^6, b_7 = \frac{x}{6} - \frac{7x^3}{6} + \frac{7x^5}{2} - \frac{7x^6}{2} + x^7,$$

$$b_8 = -\frac{1}{30} + \frac{2x^2}{3} - \frac{7x^4}{3} + \frac{14x^6}{3} - 4x^7 + x^8,$$

$$b_9 = -\frac{3x}{10} + 2x^3 - \frac{21x^5}{5} + 6x^7 - \frac{9x^8}{2} + x^9,$$

$$b_{10} = \frac{5}{66} - \frac{3x^2}{2} + 5x^4 - 7x^6 + \frac{15x^8}{2} - 5x^9 + x^{10}, \dots,$$

Theorem 1: *Let H be a Hilbert space and W be a closed subspace of H such that dim $W < \infty$ and $\{w_1, w_2, ..., w_n\}$ is any basis for W. Let $g \in H$ be arbitrary and g_0 be the unique best approximation to g out of W. Then*[45]

$$\|g - g_0\|_2 = G_g, \text{ Where } G_g = \left(\frac{Z(g, w_1, w_2, ... w_n)}{Z(g, w_1, w_2, ... w_n)}\right)^{\frac{1}{2}} \text{ and } Z \text{ is}$$

introduced in [49] as follows:

$$Z, (g, w_1, w_2, ... w_n)$$
$$= \begin{vmatrix} <g,g> & <g,w_1> & ... & <g,w_n> \\ <w_1,g> & <w_1,w_1> & ... & <w_1,w_n> \\ ... & ... & ... & ... \\ <w_n,g> & <w_n,w_1> & ... & <w_n,w_n> \end{vmatrix}.$$

Theorem 2: *Suppose $f : [0,1] \to R, f \in L^2[0,1]$ and $Y = span\{\psi_{10}(t), \psi_{11}(t), ..., \psi_{2^{k-1}M-1}(t)\}$. If $C^T\psi(t)$ is the best approximation of f out of Y, then the error bound is given by:*

$$\left\| \int_0^t f(t') \, dt' - C^T P\psi(t) \right\|_2 \leq G_f + \gamma_f$$

where, $\gamma_f = \frac{M_1}{2^{k-1}M} \sum_{n=1}^{2^{k-1}} |c_{n,M-1}|$, with $M_1 = \max_{t \in [0,1]} |\psi_{nM-1}|$, $n = 1, ..., 2^{k-1}$.

Theorem 3: *Let $L^2[0,1]$ be the Hilbert space generated by the Bernoulli wavelet basis. Let $\eta(x)$ be the continuous bounded*

function in $L^2[0,1]$. Then the Bernoulli wavelet expansion of $\eta(x)$ converges to it.

Proof: Let $\eta : [0,1] \to R$ be a continuous function and $|\eta(x)| \leq \mu$, where μ be any real number. Then Bernoulli wavelet expansion of $y(x)$ is as follows,

$$\eta(x) = \sum_{n=1}^{2^{\frac{k-1}{2}}} \sum_{m=0}^{M-1} a_{n,m} \theta_{n,m}(x).$$

$a_{n,m} = \langle \eta(x), \theta_{n,m}(x) \rangle$ denotes inner product.

$$a_{n,m} = \int_0^1 \eta(x) \theta_{n,m}(x) \, dx.$$

Since $\theta_{n,m}$ are the orthogonal basis.

$$a_{n,m} = \int_I \eta(x) \frac{2^{\frac{k-1}{2}}}{\sqrt{\frac{(-1)^{m-1}(m!)^2 \alpha_{2m}}{(2m)!}}} \beta_m(2^{k-1}x - n + 1) \, dx,$$

where, $I = \left[\frac{n-1}{2^{k-1}}, \frac{n}{2^{k-1}}\right)$.

The substitute $2^{k-1}x - n + 1 = y$ then we get,

$$a_{n,m} = \frac{2^{\frac{k-1}{2}}}{\sqrt{\frac{(-1)^{m-1}(m!)^2 \alpha_{2m}}{(2m)!}}} \int_0^1 \eta\left(\frac{y+n-1}{2^{k-1}}\right) \beta_m(y) \frac{dy}{2^{k-1}},$$

$$a_{n,m} = \frac{2^{\frac{1-k}{2}}}{\sqrt{\frac{(-1)^{m-1}(m!)^2 \alpha_{2m}}{(2m)!}}} \int_0^1 \eta\left(\frac{y+n-1}{2^{k-1}}\right) \beta_m(y) \, dy.$$

By generalized mean value theorem,

$$a_{n,m} = \frac{2^{\frac{-k+1}{2}}}{\sqrt{\frac{(-1)^{m-1}(m!)^2 \alpha_{2m}}{(2m)!}}} \eta\left(\frac{\xi+n-1}{2^{k-1}}\right) \int_0^1 \beta_m(y) \, dy, \text{ for some}$$

$\xi \in (0,1)$,

Since $\beta_m(y)$ is a bounded continuous function. Put $\int_0^1 \beta_m(y) \, dy = h$,

$$|a_{n,m}| = \left| \frac{2^{\frac{-k+1}{2}}}{\sqrt{\frac{(-1)^{m-1}(m!)^2 \alpha_{2m}}{(2m)!}}} \right| \left| \eta\left(\frac{\xi+n-1}{2^{k-1}}\right) \right| h.$$

Since, η is bounded

Hence, $|a_{n,m}| = \left| \frac{2^{\frac{-k+1}{2}} \mu h}{\sqrt{\frac{(-1)^{m-1}(m!)^2 \alpha_{2m}}{(2m)!}}} \right|.$

Therefore, $\sum_{n,m=0}^{\infty} a_{n,m}$ is absolutely convergent. Hence the Bernoulli wavelet series expansion of $\eta(x)$ converges uniformly to it.

4 Functional matrix of Bernoulli wavelets

Bernoulli wavelet basis at $k = 1$ is as follows:

$\theta_{1,0}(x) = 1,$

$\theta_{1,1}(x) = \sqrt{3}(-1 + 2x),$

$\theta_{1,2}(x) = \sqrt{5}(1 - 6x + 6x^2),$

$\theta_{1,3}(x) = \sqrt{210}(x - 3x^2 + 2x^3),$

$\theta_{1,4}(x) = 10\sqrt{21}\left(-\frac{1}{30} + x^2 - 2x^3 + x^4\right),$

$\theta_{1,5}(x) = \sqrt{\frac{462}{5}}(-x + 10x^3 - 15x^4 + 6x^5),$

$\theta_{1,6}(x) = \sqrt{\frac{1430}{691}}(1 - 21x^2 + 105x^4 - 126x^5 + 42x^6),$

$\theta_{1,7}(x) = 2\sqrt{\frac{143}{7}}(x - 7x^3 + 21x^5 - 21x^6 + 6x^7),$

$\theta_{1,8}(x) = \sqrt{\frac{7293}{3617}}(-1 + 20x^2 - 70x^4 + 140x^6 - 120x^7 + 30x^8),$

$\theta_{1,9}(x) = \sqrt{\frac{1939938}{219335}}(-3x + 20x^3 - 42x^5 + 60x^7 - 45x^8 + 10x^9),$

$\theta_{1,10}(x) = 22\sqrt{\frac{125970}{174611}}\left(\frac{5}{66} - \frac{3x^2}{2} + 5x^4 - 7x^6 + \frac{15x^8}{2} - 5x^9 + x^{10}\right),$

$\theta_{1,11}(x) = 2\sqrt{\frac{676039}{854513}}(5x - 33x^3 + 66x^5 - 66x^7 + 55x^9 - 33x^{10} + 6x^{11}).$

where,

$\theta_{10}(x) = [\theta_{1,0}(x), \theta_{1,1}(x), \theta_{1,2}(x), \theta_{1,3}(x), \theta_{1,4}(x), \theta_{1,5}(x), \theta_{1,6}(x), \theta_{1,7}(x), \theta_{1,8}(x), \theta_{1,9}(x)]^T.$

$$\int_0^x \theta_{1,1}(x)dx = \left[-\frac{1}{2\sqrt{3}}\ \ 0\ \ \frac{1}{2\sqrt{15}}\ \ 0\ 0\ 0\ 0\ 0\ 0\right]\theta_{10}(x),$$

$$\int_0^x \theta_{1,2}(x)dx = \left[0\ \ 0\ \ 0\ \ \frac{1}{\sqrt{42}}\ \ 0\ 0\ 0\ 0\ 0\right]\theta_{10}(x),$$

$$\int_0^x \theta_{1,3}(x)dx = \left[\frac{\sqrt{7}}{2\sqrt{30}}\ \ 0\ \ 0\ \ 0\ \ \frac{1}{2\sqrt{10}}\ \ 0\ 0\ 0\ 0\right]\theta_{10}(x),$$

$$\int_0^x \theta_{1,4}(x)dx = \left[0\ \ 0\ \ 0\ \ 0\ \ 0\ \ \frac{\sqrt{5}}{3\sqrt{22}}\ \ 0\ 0\ 0\ 0\right]\theta_{10}(x),$$

$$\int_0^x \theta_{1,5}(x)dx = \left[-\sqrt{\frac{11}{210}}\ \ 0\ 0\ 0\ 0\ 0\ \frac{\sqrt{691}}{10\sqrt{273}}\ \ 0\ 0\ 0\right]\theta_{10}(x),$$

$$\int_0^x \theta_{1,6}(x)dx = \left[0\ 0\ 0\ 0\ 0\ 0\ 0\ \sqrt{\frac{35}{1382}}\ \ 0\ 0\right]\theta_{10}(x),$$

$$\int_0^x \theta_{1,7}(x)dx = \left[\frac{\sqrt{143}}{20\sqrt{7}}\ \ 0\ 0\ 0\ 0\ 0\ 0\ \frac{\sqrt{3617}}{20\sqrt{357}}\ \ 0\right]\theta_{10}(x),$$

$$\int_0^x \theta_{1,8}(x)dx = \left[0\ \ 0\ \ 0\ \ 0\ 0\ 0\ 0\ 0\ 0\ 0\ \frac{\sqrt{219335}}{3\sqrt{962122}}\right]\theta_{10}(x),$$

$$\int_0^x \theta_{1,9}(x)dx = \left[-\sqrt{\frac{146965}{2895222}}\ \ 0\ 0\ 0\ 0\ 0\ 0\ 0\ 0\ 0\ 0\ 0\ 0\right]$$

$$\theta_{10}(x) + \frac{\sqrt{1222277}}{10\sqrt{482537}}\theta_{1,10}(x).$$

Integrating the above first ten basis concerning x limit from 0 to x, then expressing as a linear combination of Bernoulli wavelet basis as

$$\int_0^x \theta_{1,0}(x)dx = \left[\frac{1}{2}\ \ \frac{1}{2\sqrt{3}}\ \ 0\ 0\ 0\ 0\ 0\ 0\ 0\right]\theta_{10}(x),$$

Hence,

$$\int_0^x \theta(x)dx = B_{10\times10}\theta_{10}(x) + \overline{\theta_{10}}(x),$$

where

$$B_{10\times10} = \begin{bmatrix} \frac{1}{2} & \frac{1}{2\sqrt{3}} & 0 & 0 & 0 & 0 & 0 & 0 & 0 & 0 \\ -\frac{1}{2\sqrt{3}} & 0 & \frac{1}{2\sqrt{15}} & 0 & 0 & 0 & 0 & 0 & 0 & 0 \\ 0 & 0 & 0 & \frac{1}{\sqrt{42}} & 0 & 0 & 0 & 0 & 0 & 0 \\ \frac{\sqrt{7}}{2\sqrt{30}} & 0 & 0 & 0 & \frac{1}{2\sqrt{10}} & 0 & 0 & 0 & 0 & 0 \\ 0 & 0 & 0 & 0 & 0 & \frac{\sqrt{5}}{3\sqrt{22}} & 0 & 0 & 0 & 0 \\ -\sqrt{\frac{11}{210}} & 0 & 0 & 0 & 0 & 0 & \frac{\sqrt{691}}{10\sqrt{273}} & 0 & 0 & 0 \\ 0 & 0 & 0 & 0 & 0 & 0 & 0 & \sqrt{\frac{35}{1382}} & 0 & 0 \\ \frac{\sqrt{143}}{20\sqrt{7}} & 0 & 0 & 0 & 0 & 0 & 0 & 0 & \frac{\sqrt{3617}}{20\sqrt{357}} & 0 \\ 0 & 0 & 0 & 0 & 0 & 0 & 0 & 0 & 0 & \frac{\sqrt{219335}}{3\sqrt{962122}} \\ -\sqrt{\frac{146965}{2895222}} & 0 & 0 & 0 & 0 & 0 & 0 & 0 & 0 & 0 \end{bmatrix},$$

$$\overline{\theta_{10}}(x) = \begin{bmatrix} 0 \\ 0 \\ 0 \\ 0 \\ 0 \\ 0 \\ 0 \\ 0 \\ 0 \\ \frac{\sqrt{1222277}}{10\sqrt{482537}}\theta_{1,10}(x) \end{bmatrix}$$

In general, the first integration of the Bernoulli wavelet can be represented as;

$$\int_0^x \theta(x)dx = B_{n\times n}\theta_n(x) + \overline{\theta_n}(x).$$

Next, integrating the above ten basis twice, we get,

$$\int_0^t\int_0^t \theta_{1,0}(t)dtdt = \left[\begin{array}{cccccccccc} \frac{1}{6} & \frac{1}{4\sqrt{3}} & \frac{1}{12\sqrt{5}} & 0 & 0 & 0 & 0 & 0 & 0 & 0 \end{array}\right]\theta_{10}(t),$$

$$\int_0^t\int_0^t \theta_{1,1}(t)dtdt = \left[\begin{array}{cccccccccc} -\frac{1}{4\sqrt{3}} & -\frac{1}{12} & 0 & \frac{1}{6\sqrt{70}} & 0 & 0 & 0 & 0 & 0 & 0 \end{array}\right]\theta_{10}(t),$$

$$\int_0^t\int_0^t \theta_{1,2}(t)dtdt = \left[\begin{array}{cccccccccc} \frac{1}{12\sqrt{5}} & 0 & 0 & 0 & \frac{1}{4\sqrt{105}} & 0 & 0 & 0 & 0 & 0 \end{array}\right]\theta_{10}(t),$$

$$\int_0^t\int_0^t \theta_{1,3}(t)dtdt = \left[\begin{array}{cccccccccc} \frac{\sqrt{7}}{4\sqrt{30}} & \frac{\sqrt{7}}{12\sqrt{10}} & 0 & 0 & 0 & \frac{1}{12\sqrt{11}} & 0 & 0 & 0 & 0 \end{array}\right]\theta_{10}(t),$$

$$\int_0^t\int_0^t \theta_{1,4}(t)dtdt = \left[\begin{array}{cccccccccc} -\frac{1}{6\sqrt{21}} & 0 & 0 & 0 & 0 & 0 & \frac{\sqrt{691}}{6\sqrt{30030}} & 0 & 0 & 0 \end{array}\right]\theta_{10}(t),$$

$$\int_0^t\int_0^t \theta_{1,5}(t)dtdt = \left[\begin{array}{cccccccccc} -\frac{\sqrt{11}}{2\sqrt{210}} & -\frac{\sqrt{11}}{6\sqrt{70}} & 0 & 0 & 0 & 0 & \frac{1}{2\sqrt{390}} & 0 & 0 \end{array}\right]\theta_{10}(t),$$

$$\int_0^t\int_0^t \theta_{1,6}(t)dtdt = \left[\begin{array}{cccccccccc} \frac{\sqrt{143}}{4\sqrt{6910}} & 0 & 0 & 0 & 0 & 0 & 0 & \frac{\sqrt{3617}}{4\sqrt{352410}} & 0 \end{array}\right]\theta_{10}(t),$$

$$\int_0^t\int_0^t \theta_{1,7}(t)dtdt = \left[\begin{array}{cccccccccc} \frac{\sqrt{143}}{40\sqrt{7}} & \frac{\sqrt{143}}{40\sqrt{21}} & 0 & 0 & 0 & 0 & 0 & 0 & \frac{\sqrt{43867}}{84\sqrt{9690}} \end{array}\right]\theta_{10}(t),$$

$$\int_0^t\int_0^t \theta_{1,8}(t)dtdt = \left[\begin{array}{cccccccccc} -\frac{5\sqrt{221}}{6\sqrt{119361}} & 0 & 0 & 0 & 0 & 0 & 0 & 0 & 0 & 0 \end{array}\right]\theta_{10}(t) + \frac{\sqrt{174611}}{6\sqrt{7559530}}\theta_{1,10}(t),$$

$$\int_0^t\int_0^t \theta_{1,9}(t)dtdt = \left[\begin{array}{cccccccccc} -\frac{\sqrt{146965}}{2\sqrt{2895222}} & -\frac{\sqrt{146965}}{6\sqrt{965074}} & 0 & 0 & 0 & 0 & 0 & 0 & 0 & 0 \end{array}\right]\theta_{10}(t) + \frac{\sqrt{77683}}{2\sqrt{30268230}}\theta_{1,11}(t).$$

Hence,

$$\int_0^t \int_0^t \theta(t)dtdt = B'_{10\times10}\theta_{10}(t) + \overline{\theta_{10}}'(t),$$

where

$$B'_{10\times10} = \begin{bmatrix} \frac{1}{6} & \frac{1}{4\sqrt{3}} & \frac{1}{12\sqrt{5}} & 0 & 0 & 0 & 0 & 0 & 0 & 0 \\ -\frac{1}{4\sqrt{3}} & -\frac{1}{12} & 0 & \frac{1}{6\sqrt{70}} & 0 & 0 & 0 & 0 & 0 & 0 \\ \frac{1}{12\sqrt{5}} & 0 & 0 & 0 & \frac{1}{4\sqrt{105}} & 0 & 0 & 0 & 0 & 0 \\ \frac{\sqrt{7}}{4\sqrt{30}} & \frac{\sqrt{7}}{12\sqrt{10}} & 0 & 0 & 0 & \frac{1}{12\sqrt{11}} & 0 & 0 & 0 & 0 \\ -\frac{1}{6\sqrt{21}} & 0 & 0 & 0 & 0 & 0 & \frac{\sqrt{691}}{6\sqrt{30030}} & 0 & 0 & 0 \\ -\frac{\sqrt{11}}{2\sqrt{210}} & -\frac{\sqrt{11}}{6\sqrt{70}} & 0 & 0 & 0 & 0 & 0 & \frac{1}{2\sqrt{390}} & 0 & 0 \\ \frac{\sqrt{143}}{4\sqrt{6910}} & 0 & 0 & 0 & 0 & 0 & 0 & 0 & \frac{\sqrt{3617}}{4\sqrt{352410}} & 0 \\ \frac{\sqrt{143}}{40\sqrt{7}} & \frac{\sqrt{143}}{40\sqrt{21}} & 0 & 0 & 0 & 0 & 0 & 0 & 0 & \frac{\sqrt{43867}}{84\sqrt{9690}} \\ -\frac{5\sqrt{221}}{6\sqrt{119361}} & 0 & 0 & 0 & 0 & 0 & 0 & 0 & 0 & 0 \\ -\frac{\sqrt{146965}}{2\sqrt{2895222}} & -\frac{\sqrt{146965}}{6\sqrt{965074}} & 0 & 0 & 0 & 0 & 0 & 0 & 0 & 0 \end{bmatrix},$$

$$\overline{\theta_{10}}'(t) = \begin{bmatrix} 0 \\ 0 \\ 0 \\ 0 \\ 0 \\ 0 \\ 0 \\ 0 \\ \frac{\sqrt{174611}}{6\sqrt{7559530}}\theta_{1,10}(t) \\ \frac{\sqrt{77683}}{2\sqrt{30268230}}\theta_{1,11}(t) \end{bmatrix}$$

In the same way, we can create matrices of various sizes for our comfort.

5 Method of solution

The semi-infinite domain $[0, \infty)$ in (23) has to be transformed to $[0, 1]$ by using the coordinate transformation $\xi = \frac{\eta}{\eta_\infty}$ and change of variable $F(\xi) = \frac{f(\eta)}{\eta_\infty}$. Under this transformation (23) becomes

$$F'''(\xi) + \eta_\infty^2 F(\xi) F''(\xi) + \beta \eta_\infty^2 \left(\in^2 -(F'(\xi))^2\right) + M^2 \eta_\infty^2 \left(\in -F'(\xi)\right) = 0. \tag{26}$$

where η_∞ is an unknown finite boundary which is assumed to satisfy the asymptotic condition $f''(\eta_\infty) = 0$. Also η_∞

varies with the parameters β, M, and $\in$. The boundary conditions (24) are transformed to

$$F(0) = 0, \qquad F'(0) = 1-\in, \qquad F'(1) = \in. \tag{27}$$

6 Numerical solution by Bernoulli wavelet collocation method (BWCM)

Consider the model

$$F'''(\xi) + \eta_\infty^2 F(\xi) F''(\xi) + \beta \eta_\infty^2 \left(\in^2 -(F'(\xi))^2\right) + M^2 \tag{28}$$

$$\eta_\infty^2 \left(\in -F'(\xi)\right) = 0,$$

with boundary conditions

$$F(0) = 0, \qquad F'(0) = 1-\in, \qquad F'(1) = \in. \tag{29}$$

Let

$$F'''(\xi) = A^T G(\xi). \tag{30}$$

Integrate (30) concerning ξ from 0 to ξ,

$$F''(\xi) = F''(0) + A^T \left(P G(\xi) + \overline{P}(\xi)\right). \tag{31}$$

Integrate (31) concerning ξ from 0 to ξ,

$$F'(\xi) = 1-\in + \xi F''(0) + A^T \left(P' G(\xi) + \overline{P}'(\xi)\right). \tag{32}$$

Integrate (32) concerning ξ from 0 to ξ,

$$F(\xi) = \xi(1-\in) + \frac{\xi^2}{2} F''(0) + A^T \left(P'' G(\xi) + \overline{P}''(\xi)\right). \tag{33}$$

Put $\xi = 1$ in (32), we get,

$$F''(0) = 2 \in -1 - A^T \left(P' \, G(\xi) + \overrightarrow{P}'(\xi) \right) |_{\xi=1}. \tag{34}$$

Fit the Eqs. (30) – (34) in Eq. (28) and discretize the resultant equation using the collocation point $\xi_i = \frac{2i-1}{2M}$ where $i = 1, 2, ..., M$ we get the M system of equations in M unknown coefficients. Solving this system by Newton Raphson method, the value of A^T is obtained. Substituting this value in Eq. (33) to get an approximate solution $F(\xi)$.

The wall shear stress or skin-friction coefficient $f''(0)$ is given by,

$$f''(0) = \frac{1}{\eta_\infty} \left[2 \in -1 - A^T \left(P' \, G(\xi) + \overrightarrow{P}'(\xi) \right) |_{\xi=1} \right]. \tag{35}$$

Fig. 1 Comparison of $f(\eta)$ with analytic solution (37) for $\beta = 1$.

7 Results and discussion

Case (i): Solution for $\in = 0$ and general β.

The two-dimensional laminar flow due to stretching sheet without magnetic field is given by [16, 17, 50],

$$f'''(\eta) + f(\eta) f''(\eta) - \beta f'(\eta)^2 = 0, \tag{36}$$

$$f(0) = 0, \; f'(0) = 1, \; f'(\infty) = 0.$$

Equation (36) has an exact solution for some particular values of β[26]:

For $\beta = 1, f(\eta) = 1 - e^{-\eta}$. \tag{37}

For $\beta = -1, f(\eta) = \sqrt{2} \tanh\left(\frac{\eta}{\sqrt{2}} \right)$. \tag{38}

Figures 1 and 2 show that the solution from BWCM coincides with the exact solution.

Case(ii): Solution for $\in = 0$ and general β and M.

The two-dimensional boundary layer flow due to the stretching plate with the magnetic field is given by [24, 25]:

$$\left.\begin{array}{l} f'''(\eta) + f(\eta) f''(\eta) - \beta f'(\eta)^2 - M^2 f'(\eta) = 0, \\ f(0) = 0, \quad f'(0) = 1, \quad f'(\infty) = 0. \end{array}\right\} \tag{39}$$

The exact solution for $\beta = 1$ and general M is given by [11]:

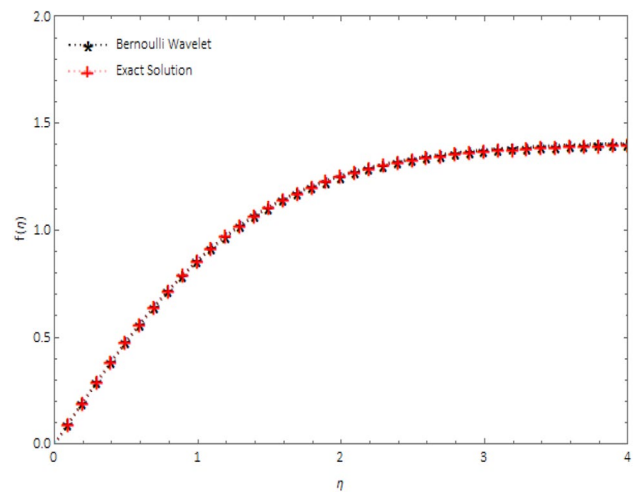$$f(\eta) = \frac{1 - e^{-\eta \sqrt{1+M^2}}}{\sqrt{1+M^2}}. \tag{40}$$

Fig. 2 Comparison of $f(\eta)$ with analytic solution (38) for $\beta = -1$.

From Table 1, we can say that BWCM yields a better solution and consumes less time when compared to the Haar wavelet method.

Figures 3 and 4 show that the basic solution and velocity profiles satisfy the solution in (40).

Case (iii): Solution for $\in = 1$ and general β and M.

This case is described by the MHD Falkner-Skan equation [4]:

$$\left.\begin{array}{l} f'''(\eta) + f(\eta) f''(\eta) + \beta \left(1 - f'(\eta)^2 \right) + M^2 \left(1 - f'(\eta) \right) = 0, \\ f(0) = 0, \quad f'(0) = 0, \quad f'(\infty) = 1. \end{array}\right\} \tag{41}$$

The velocity profile $f'(\eta)$ and shear flow $f''(\eta)$ for the various values of pressure gradient β with and without magnetic field are shown in Figs. 5 and 6. It is noted

Table 1 Comparison of values of $f''(0)$ for $\beta = 1$ and different values of M

M^2	BWCM	Haar wavelet ($J=6$)	Exact[11]	BWCM computation time	Haar wavelet computation time
0	− 1.00006	− 0.99594	− 1	1.11	10.468
0.1	− 1.04883	− 1.04542	− 1.04881	1.062	10.874
0.2	− 1.09545	− 1.09264	− 1.09545	0.969	10.843
0.3	− 1.14017	− 1.13787	− 1.14018	1.079	10.797
0.4	− 1.1832	− 1.18131	− 1.18322	1.109	10.858
0.5	− 1.22472	− 1.22315	− 1.22474	1.219	10.94
0.6	− 1.26488	− 1.26356	− 1.26491	1.047	10.562
0.7	− 1.30379	− 1.30268	− 1.30384	1.156	10.829
0.8	− 1.34158	− 1.34062	− 1.34641	1.047	10.703
0.9	− 1.37832	− 1.37749	− 1.37840	1.094	10.719
1.0	− 1.41411	− 1.41338	− 1.41421	1.047	10.812
2.0	− 1.73138	− 1.73129	− 1.73205	1.141	10.844
3.0	− 1.9977	− 1.99892	− 2	1.157	10.579
4.0	− 2.23064	− 2.23457	− 2.23607	1.249	10.53
5.0	− 2.43885	− 2.44751	− 2.44949	1.218	10.656
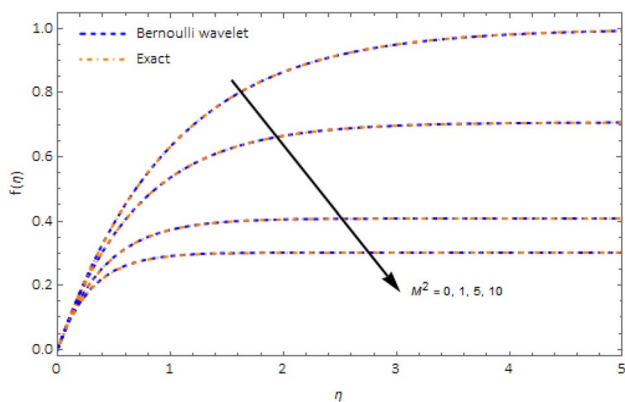
Fig. 3 Comparison of solution $f(\eta)$ with analytic solution (40) for different magnetic parameters
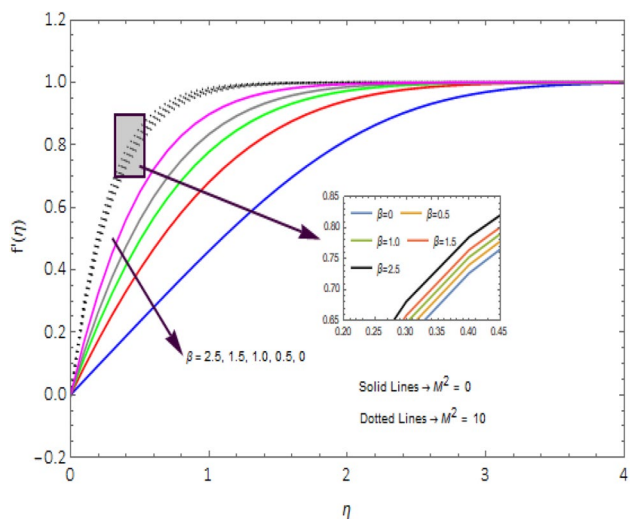
Fig. 5 Variation of velocity profiles for various values of β and M in (41)
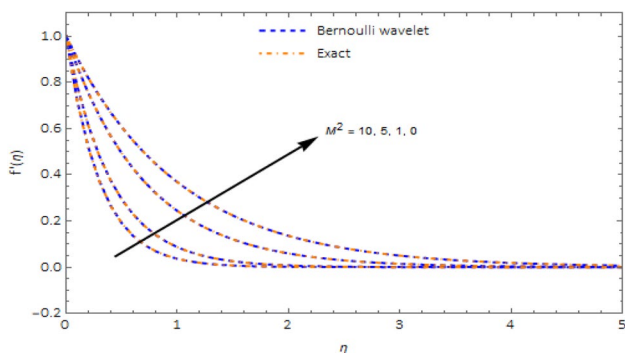
that as the pressure gradient β increases from zero, the boundary-layer thickness becomes smaller and smaller. The boundary-layer thickness further becomes smaller in the presence of the magnetic field because more energy is released into the flow by the applied magnetic which accelerates the motion of the fluid particles, hence fluid particles move faster. Further increase in M makes the flow more stable. From the Fig. 6, we can also observe that in both cases $M^2 = 0$ and $M^2 = 10$ $f''(\eta)$ asymptotically tends to zero as $\eta \to \infty$.

Fig. 4 Comparison of solution $f'(\eta)$ with analytic solution (40) for different magnetic parameters

Fig. 6 Shear stress profiles for various values of β and M in (41)
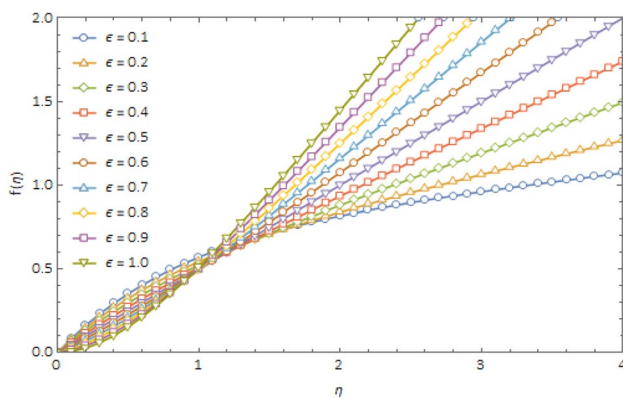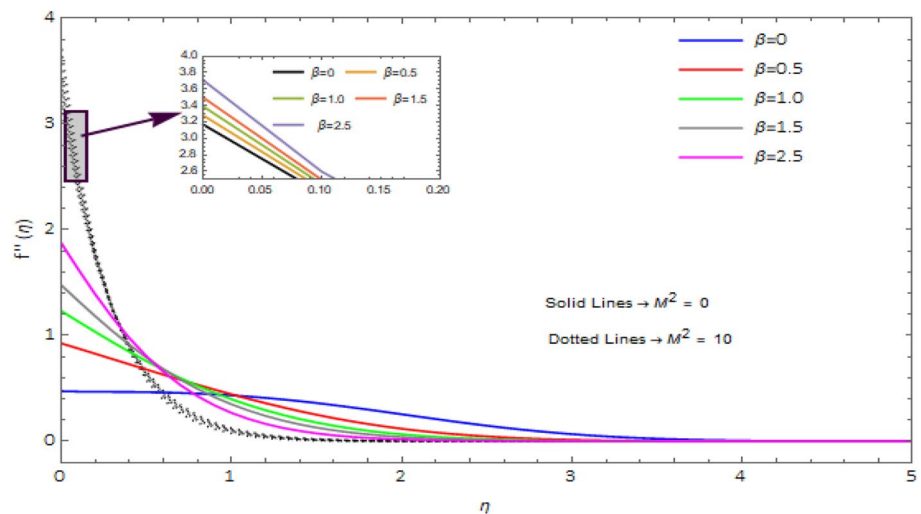

Fig. 7 Graph of solution $f(\eta)$ for the class of the Falkner-Skan problem at $\beta = 1.5, M^2 = 0$ and different values of $\in$
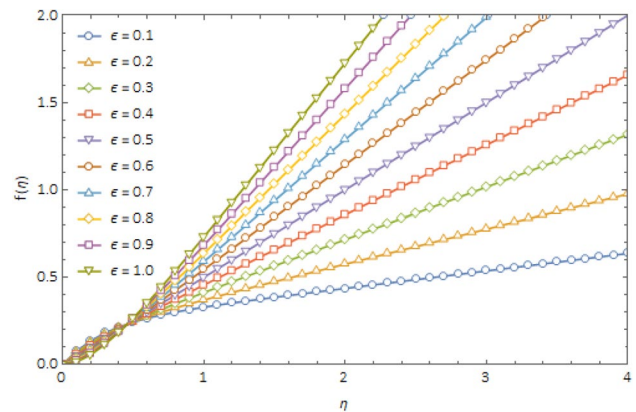

Fig. 8 Graph of solution $f(\eta)$ for the class of the Falkner-Skan problem at $\beta = 1.5, M^2 = 10$ and different values of $\in$

Case (iv): Solution for $0 < \in < 1$ and general β and M.

The basic solution $f(\eta)$ is calculated for two sets of values of M (without magnetic field and with magnetic field) and different values of $\in$ which are shown in Figs. 7 and 8. Figures 9 and 10 are obtained by taking $\beta = -1$ and $\beta = -0.4$ are the same as those produced in [17]. Also, when $M^2 = 0$, the velocity profiles experience both undershoots and overshoots near the wedge, and when $M^2 > 0$, the flow becomes more stable. As the magnetic field increases, the point of intersection of these solutions is very much closer to the wedge surface. It is seen that when $M^2 = 0$ the thickness of the boundary layer is a little large when compared to $M^2 = 10$ because the magnetic field releases the energy to flow, thereby making the fluid particles move fast; as a result, the boundary-layer thickness becomes small and makes the flow more stable and mild. It is also seen that as β increases from negative ($\beta = -1, -0.4$) to positive ($\beta = 0.5, 1.5$), the
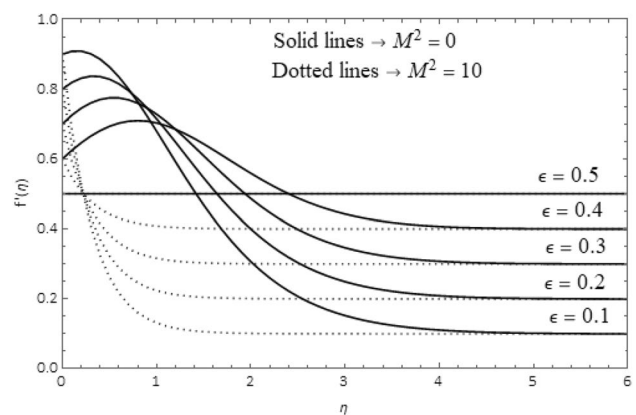

Fig. 9 Variation of a velocity profile for $\beta = -1$ in the absence (first set of solution) and presence of the magnetic field

undershoots $\left(f'(\eta) < \in\right)$ and overshoots $\left(f'(\eta) > \in\right)$ vanishes and the flow become mild. This is seen in Figs. 11
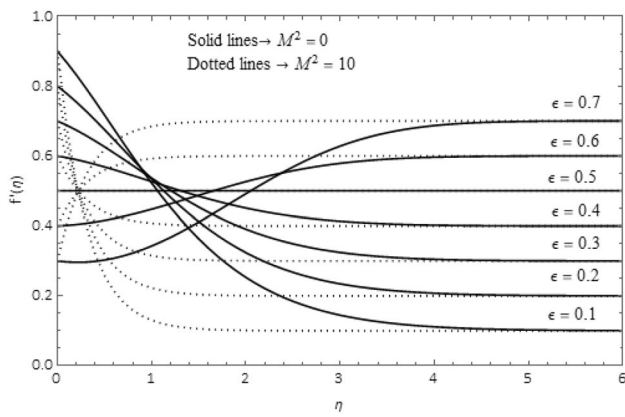
Fig. 10 Variation of a velocity profile for $\beta = -0.4$ in the absence and presence of the magnetic field
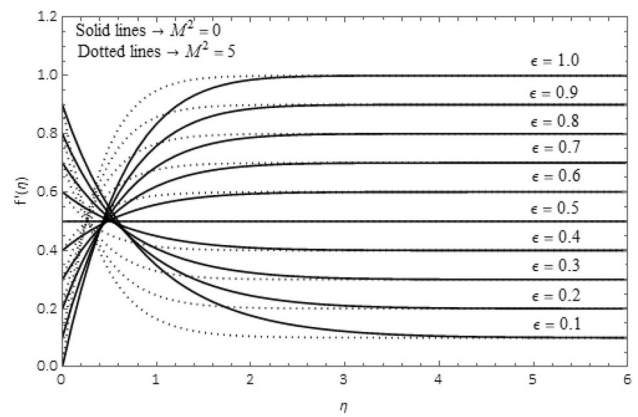

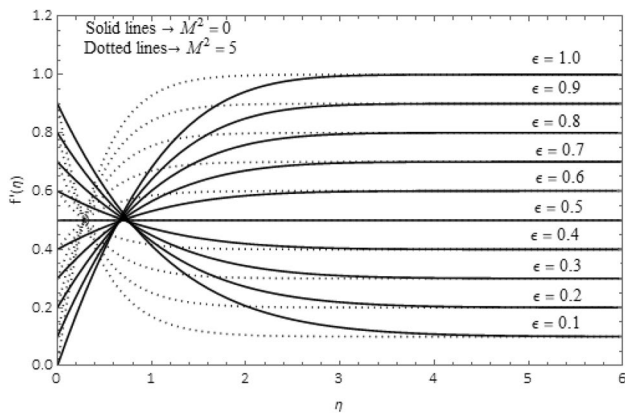**Fig. 12** Velocity profiles with and without magnetic field at $\beta = 1.5$

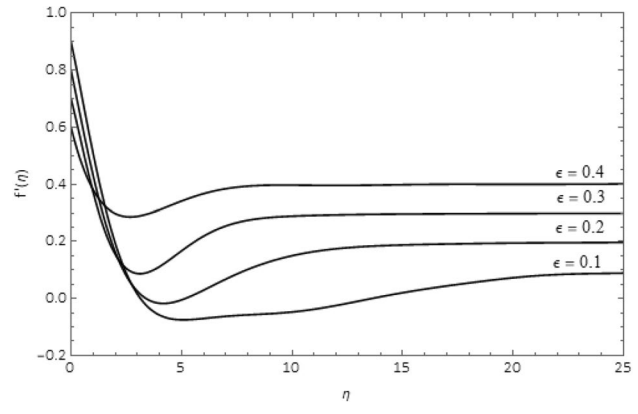**Fig. 11** Velocity profiles with and without magnetic field at $\beta = 0.5$

Fig. 13 Variation of velocity profiles for $\beta = -1$ in the absence of magnetic field (second set solutions)

and 12 for two different values of *M*. Also, the point of intersection is still nearer to the wedge surface because the flow is accelerated, and the boundary layer thickness becomes smaller and smaller. In addition to this, we can notice that when $\in > \frac{1}{2}$ and $\in < \frac{1}{2}$, all the velocity profiles move toward the endpoints. From Fig. 13, we can say BWCM successfully predicts the double solution for some set of physical parameters when η_∞ is taken to be as large as possible. The double solution is observed only in the absence of a magnetic field, and in the presence of a magnetic field, we found only a single solution.

8 Conclusion

In this study, we developed a new operational matrix of integration by the Bernoulli wavelet and the new technique called BWCM. This proposed method studied the two-dimensional boundary layer flow of viscous fluid in the presence of a magnetic field. As we know, many semi-analytical techniques are needed for small parameters, but such difficulties don't arise in the proposed technique. Here, we found the wavelet solution, including the double solution, by varying the parameters such as, $\in$, β, and M. The following are the important findings from this study:

- As the pressure gradient β increases from zero, the boundary-layer thickness becomes smaller and smaller. The boundary-layer thickness further becomes smaller in the presence of the magnetic field *M*.
- The velocity profile experiences both overshoots and undershoots and vanishes when β increases from negative to positive.

- Dual solutions are observed only in the absence of the magnetic field. In the presence of a magnetic field, we found only one solution.

Declarations

Conflict of interest On behalf of all authors, the corresponding author states that there is no conflict of interest.

References

1. Sakiadis BC (1961) Boundary-layer behavior on continuous solid surfaces: II The boundary layer on a continuous flat surface. AIChE J 7:221–225
2. Datta BK (2003) Analytic solution for the Blasius equation. Indian J Pure Appl Math 34(2):237–240
3. Abbasbandy S (2007) A numerical solution of Blasius equation by Adomians decomposition method and comparison with homotopy perturbation method. Chaos, Solitons Fractals 31(1):257–260
4. Abbasbandy S, Hayat T (2009) Solution of the MHD Falkner-Skan flow by Hankel-Pade method. Phys Lett A 373(7):731–734
5. Abbasbandy S, Hayat T (2009) Solution of the MHD Falkner-Skan flow by homotopy analysis method. Commun Nonlinear Sci Numer Simul 14(910):3591–3598
6. Khan M, Gondal MA, Hussain I, Vanani SK (2012) A new comparative study between homotopy analysis transform method and homotopy perturbation transform method on a semi-infinite domain. Math Comput Model 55(3):1143–1150
7. Zeb H, Bhatti S, Khan U, Wahab HA, Mohamed A, Khan I (2022) Impact of homogeneous-heterogeneous reactions on flow of Non-Newtonian ferrofluid over a stretching sheet. J Nanomater 2022:11
8. Anusha T, Mahabaleshwar US, Sheikhnejad Y (2022) An MHD of nanofluid flow over a porous stretching/shrinking plate with mass transpiration and Brinkman ratio. Transp Porous Med 142:333–352
9. Liao S (1999) A uniformly valid analytic solution of two-dimensional viscous flow over a semi-infinite flat plate. J Fluid Mech 385:101–128
10. Liao S (2005) A new branch of solutions of boundary-layer flows over an impermeable stretched plate. Int J Heat Mass Transf 48(12):2529–2539
11. Liao SJ (2003) On the analytic solution of magnetohydrodynamic flows of non-Newtonian fluids over a stretching sheet. J Fluid Mech 488:189–212
12. Asaithambi A (2004) A second-order finite-difference method for the Falkner-Skan equation. Appl Math Comput 156(3):779–786
13. Asaithambi A (2005) Solution of the Falkner-Skan equation by recursive evaluation of Taylor coefficients. J Comput Appl Math 176(1):203–214
14. Kudenatti RB, Kirsur SR, Achala L, Bujurke N (2013) Exact solution of two-dimensional MHD boundary layer flow over a semi-infinite flat plate. Commun Nonlinear Sci Numer Simul 18(5):1151–1161
15. Kudenatti RB, Kirsur SR, Achala L, Bujurke N (2013) MHD boundary layer flow over a non-linear stretching boundary with suction and injection. Int J Non-Linear Mech 50:58–67
16. Kudenatti RB, Awati VB, Bujurke N (2011) Approximate analytical solutions of a class of boundary layer equations over nonlinear stretching surface. Appl Math Comput 218(6):2952–2959
17. Kudenatti RB (2012) A new exact solution for boundary layer flow over a stretching plate. Int J Non-Linear Mech 47(7):727–733
18. Sachdev PL, Kudenatti RB, Bujurke NM (2008) Exact analytic solution of a boundary value problem for the Falkner-Skan equation. Stud Appl Math 120(1):1–16
19. Chakrabarti A, Gupta AS (1979) Hydromagnetic flow and heat transfer over a stretching sheet. Q Appl Math 37(1):73–78
20. Chiam TC (1995) Hydromagnetic flow over a surface stretching with a power-law velocity. Int J Eng Sci 33(3):429–435
21. Uddin MJ, Beg OA, Amin N (2014) Hydromagnetic transport phenomena from a stretching or shrinking nonlinear nanomaterial sheet with Navier slip and convective heating: a model for bio-nano-materials processing. J Magn Magn Mater 368:252–261
22. Uddin MJ, Kabir MN, Alginahi YM (2015) Lie group analysis and numerical solution of magnetohydrodynamic free convective slip flow of micropolar fluid over a moving plate with heat transfer. Comput Math Appl 70(5):846–856
23. Uddin MJ, Beg OA, Uddin MN (2016) Energy conversion under conjugate conduction, magneto-convection, diffusion and nonlinear radiation over a non-linearly stretching sheet with slip and multiple convective boundary conditions. Energy 115:1119–1129
24. Hayat T, Hussain Q, Javed T (2009) The modified decomposition method and pade approximants for the MHD flow over a non-linear stretching sheet. Nonlinear Anal Real World Appl 10(2):966–973
25. Rashidi MM (2009) The modified differential transform method for solving MHD boundary-layer equations. Comput Phys Commun 180(11):2210–2217
26. Karkera H, Katagi NN, Kudenatti RB (2020) Analysis of general unified MHD boundary-layer flow of a viscous fluid - a novel numerical approach through wavelets. Math Comput Simul 168:135–154
27. Mishra V (2011) Haar wavelet approach to fluid flow between parallel plates. Int J Fluids Eng 3(4):403–410

28. Najeeb AK, Faqiha S, Amber S et al (2016) Haar wavelet solution of the MHD Jeffery Hamel flow and heat transfer in Eyring Powell fluid. AIP Adv 6:115102

29. Awati VB, Mahesh KN, Wakif A (2021) Haar wavelet scrutinization of heat and mass transfer features during the convective boundary layer flow of a nanofluid moving over a nonlinearly stretching sheet. Partial Differential Equ Appl Math 4:100192

30. Aznam SM, Ghani N, Chowdhury MSH (2019) A numerical solution for nonlinear heat transfer of fin problems using the Haar wavelet quasilinearization method. Results Phys 14:102393

31. Islam S, Bozidar S, Imran A, Fazal-i-Haq (2011) Haar wavelet collocation method for the numerical solution of boundary layer fluid flow problems. Int J Thermal Sci 50:686–697

32. Maan H, Mishra V, Mittal RC (2013) Numerical solution of a laminar viscous flow boundary layer equation using uniform Haar wavelet Quasi-linearization Method. World Acad Sci Eng Technol J 79:1410–1417

33. Karkera H, Katagi NN (2021) Wavelet-based numerical solution for mhd boundary-layer flow due to stretching sheet. Int J Appl Mech Eng 26(3):84–103

34. Vishwanath AB, Mahesh Kumar N (2021) Analysis of forced convection boundary layer flow and heat transfer past a semi-infinite static and moving flat plate using nanofluids-by Haar wavelets. J Nanofluids 10(1):106–117

35. Siri Z, Ghani NAC, Kasmani RM (2018) Heat transfer over a steady stretching surface in the presence of suction. Boundary Value Problems, p 126

36. Kaur H, Mishra V, Mittal R (2013) Numerical solution of a laminar viscous flow boundary layer equation using uniform Haar wavelet quasi-linearization method, world academy of science, engineering and technology, open science index 79. Int J Math Comput Sci 7(7):1199–1204

37. Usman M, Zubair T, Hamid M, Ul Haq R, Khan ZH (2021) Unsteady flow and heat transfer of tangent-hyperbolic fluid: Legendre wavelet-based analysis. Heat Transfer 50:3079–3093

38. Kumbinarasaiah S, Raghunatha KR (2021) The applications of Hermite wavelet method to nonlinear differential equations arising in heat transfer. Int J Thermofluids 9:100066

39. Rahimkhani P, Ordokhani Y, Babolian E (2017) A new operational matrix based on Bernoulli wavelets for solving fractional delay differential equations. Numerical Algorithms 74:223–245

40. Rahimkhani P, Ordokhani Y, Babolian E (2017) Numerical solution of fractional pantograph differential equations by using generalized fractional-order Bernoulli wavelet. J Comput Appl Math 309:493–510

41. Adel W, Sabir Z (2020) Solving a new design of nonlinear second-order Lane-Emden pantograph delay differential model via Bernoulli collocation method. Eur Phys J Plus 135:1–12

42. Lal S, Kumar S (2021) Approximation of functions by Bernoulli wavelet and its applications in solution of Volterra integral equation of second kind. Arab J Math. https://doi.org/10.1007/s40065-021-00351-z

43. Sahu PK, Saha Ray S (2017) A new Bernoulli wavelet method for numerical solutions of nonlinear weakly singular volterra integro-differential equations. Int J Comput Methods 14:03

44. Balaji S (2016) A new Bernoulli wavelet operational matrix of derivative method for the solution of nonlinear singular Lane-Emden type equations arising in astrophysics. J Comput Nonlinear Dyn. https://doi.org/10.1115/1.4032386

45. Keshavarz E, Ordokhani Y, Razzaghi M (2014) Bernoulli wavelet operational matrix of fractional order integration and its applications in solving the fractional-order differential equations. Appl Math Model 38:6038–6051

46. Elham KH, Ordokhani Y, Mohsen R (2019) The Bernoulli wavelets operational matrix of integration and its applications for the solution of linear and nonlinear problems in calculus of variations. Appl Math Comput 351:83–98

47. Sahlan MN, Afshari H, Alzabut J, Alobaidi G (2021) Using fractional Bernoulli wavelets for solving fractional diffusion wave equations with initial and boundary conditions. Fractal Fract 5:212

48. Yuan SW (1976) Foundations of fluid mechanics. PHI Priv. Limited, London

49. Kumbinarasaiah S, Raghunatha KR (2022) Study of special types of boundary layer natural convection flow problems through the clique polynomial method. Heat Transfer 51:434–450

50. Sachdev P, Bujurke N, Awati V (2005) Boundary value problems for third-order nonlinear ordinary differential equations. Stud Appl Math 115:303–318

Publisher's Note Springer Nature remains neutral with regard to jurisdictional claims in published maps and institutional affiliations.